https://doi.org/10.15407/ujpe68.7.474

V. MYSTETSKYI,[1] S. BUGAYCHUK [1, 2]

[1] Institute of Physics, Nat. Acad. of Sci. of Ukraine
(46, Nauky Ave., Kyiv 03028, Ukraine; e-mail: misteckiyviktor@ukr.net)
[2] Faculté de Physique, Laboratoire PhLAM, l'Université de Lille
(42, Rue Paul Duez, 59000 Lille, France)

CONTROL OVER LASER BEAM INTENSITIES IN LIQUID CRYSTAL VALVES WHEN RECORDING DYNAMIC VOLUME GRATINGS

Experimental studies of dynamic holography in pure nematic liquid crystals (NLCs) confirm the recording of dynamic gratings not only in NLC cells with homeotropic orientation, but also in planar ones. The explanation can be found on the basis of the photorefractive mechanism of grating recording, which is characterized by the formation of an unbalanced charge at the cell substrate surface under the action of spatially inhomogeneous light beams. The emergence of an internal tangential electric field (along the cell substrate) together with an external electric field applied normally to the cell substrates makes it possible to control the direction of the net electric field vector. In this paper, a model describing how the intensities of laser beams change at their self-diffraction and diffraction at a dynamic grating generated in the NLC has been developed and analyzed. The dynamic phase grating appears due to the orientation mechanism of birefringence in the NLC at the mixing of two laser beams that form a spatially periodic interference pattern of the acting light field. The results of calculations of the output laser beam intensities in the first self-diffraction and diffraction orders are in good agreement with experimental data. In particular, they explain a well-pronounced maximum in the dependence of the diffraction efficiency on the external applied voltage.

K e y w o r d s: nematic liquid crystals, two-wave mixing, dynamic gratings, diffraction efficiency.

1. Introduction

Liquid crystal (LC) materials and their composites are considered as promising nonlinear optical materials for modern optoelectronic systems. They find a lot of applications, in particular, for displays, spatial light modulators, sensors, adaptive optical elements, and many others [1–4]. In nonlinear photonic systems, such a phenomenological effect is used, as a variation in the refractive index of LC materials under either the action of light or the simultaneous action of laser beams and an electric field. The effect is based on the mechanism of collective reorientation of molecules in the LC cell, which is easily controlled by external factors and results in the refractive index change. The methods of dynamic holography are among the promising ones for transforming the parameters of laser beams and images. They cover many applications: the control over laser beam parameters

C i t a t i o n: Mystetskyi V., Bugaychuk S. Control over laser beam intensities in liquid crystal valves when recording dynamic volume gratings. *Ukr. J. Phys.* **68**, No. 7, 474 (2023). https://doi.org/10.15407/ujpe68.7.474.

Ц и т у в а н н я: Мистецький В.А., Бугайчук С.А. Керування інтенсивністю лазерного випромінювання у рідкокристалічних вентилях при записі об'ємної динамічної ґратки. *Укр. фіз. журн.* **68**, №7, 476 (2023).

[5,6]; the development of various sensors [7–9]; optical phase conjugation (OPC), which is used to create mirrors with an inverted wavefront, which is very necessary for lidar systems and photolithography [10]; the development of systems for optical computing; and the creation of optical computers and holographic artificial intelligence [11, 12].

In this paper, we consider the effects of controlling the intensities of the output laser beams at the two-wave mixing in nematic liquid crystals (NLCs). The main mechanism consists in recording the dynamic grating of the refractive index under the action of a periodic interference field that is formed by two incoming laser beams, followed by the self-diffraction of the recording laser beams or the diffraction of the test beam at the dynamic grating. Here, we consider the photorefractive mechanism of optical nonlinearity and the formation of a dynamic phase grating in the LC. The specific feature is the creation of the internal field of a space charge, which reorients the LC molecules [13, 14]. This approach is very promising, because the unbalanced charge is formed on a cell substrate under the action of a spatially inhomogeneous light field. As a result, the director reorientation begins from the surface of this substrate and spreads into the cell volume [15]. Confinement effects such as an enhancement of the local field factor and a diminishing of the working volume for the reorientation of LC molecules [16, 17] are appreciable for the LC near this surface, which allows a substantial reduction of the relaxation time with the simultaneous growth of nonlinear refractive index [18–22].

We present a computer simulation of various scenarios for controlling the intensity of laser beams in NLCs at the two-wave mixing. The mathematical model for calculating the parameters of the diffraction and self-diffraction at a dynamic grating is considered in detail for NLC cells with homeotropic and planar molecular orientations. An important new result of this work consists in that we obtained optimal values for the reorientation angle of the LC director, at which the maximum diffraction efficiency is observed. Those values are different for cells with homeotropic and planar orientations. The developed model also makes it possible to consider the photorefractive recording mechanism of dynamic gratings and to estimate the magnitudes of the internal electric fields required for the implementation of those scenarios.

2. The Model of Wave Diffraction and Self-Diffraction at Dynamic Gratings in Planar NLC Cells

2.1. S-effect in a planar NLC cell

As a rule, the reorientation of the NLC director in the cell bulk is considered in the approximation of ideal nematic single crystal. In this approximation, it is assumed that the molecules are on average oriented along the general direction $\pm\mathbf{d}$, where $\mathbf{d}$ is a unit vector describing the direction of the LC director. The system is uniaxial, and the order parameter is a tensor [23]. The standard approach consists in considering the LC as an anisotropic liquid that exhibits both elastic and viscous properties [3, 23].

If an electric field is applied to the cell, the director inclination angle changes. The electric field $\mathbf{E}$ creates a torque for the LC director. LCs demonstrate many interesting electro-optical effects that have no analogs in solid and liquid materials. This is a result of a high lability of the LC structure: low external electric fields lead to substantial transformations of the director field and, accordingly, to changes in the optical properties of LCs. At low electric voltages near the critical Fréedericksz transition, the nematic molecules become reoriented, and, eventually, the director gets oriented along the external electric field, if $\Delta\varepsilon > 0$ or perpendicularly to the field, if $\Delta\varepsilon < 0$. Since the nematic is optically anisotropic (positive), the position of the optical indicatrix with respect to the electric field and light directions changes. Such electro-optical effects caused by the reorientation owing to Fréedericksz transition are called orientational [3, 24]. These effects have magnetic analogs.

In the framework of the continuum theory of nematics, when only short-range intermolecular forces are taken into consideration, the following Frank constants are used to describe the transformations of the NLC director: K_1 is the splay modulus ($\operatorname{div}\mathbf{d} \neq 0$), K_2 is the twist modulus ($\mathbf{d}\cdot\operatorname{rot}\mathbf{d} \neq 0$), and K_3 is the bend modulus ($\mathbf{d}\times\operatorname{rot}\mathbf{d} \neq 0$).

Consider the standard sandwich-like geometry of a cell with a nematic LC. Its simplest two-dimensional model is exhibited in Fig. 1. A nematic layer of thickness L is located between two substrates that are infinite along the x- and y-axes. A two-dimensional (2D) system is considered, where the director $\mathbf{d}$ is located in the plane (z, x). Rod-shaped mesogenic

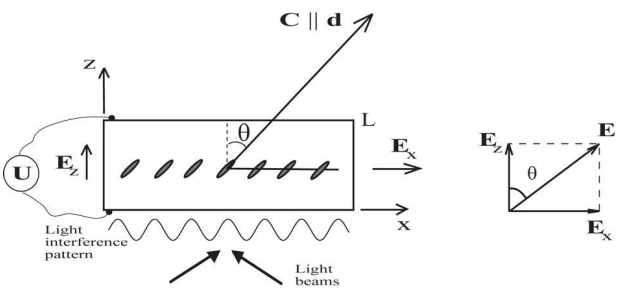

Fig. 1. Schematic diagram of a uniaxial nematic liquid crystal medium; θ is the tilt angle of the LC director with respect to the z-axis; $\mathbf{d}$ is the LC director demonstrating the predominant orientation of the long axes of the LC molecules, the vector $\mathbf{C}$ marks the optical axis of the LC medium, L is the LC cell thickness, vector $\mathbf{E}_z$ is the external electric field created by the voltage U applied to the cell substrates, and vector $\mathbf{E}_x$ is the internal electric field created by an unbalanced charge

LC molecules are characterized by positive optical anisotropy. The director vector determines the direction of the NLC optical axis $\mathbf{C}$: $\mathbf{C} \parallel \mathbf{d}$. We assume that the director $\mathbf{d}$ determines the orientation of LC molecules only in the cell bulk; the surface reorientation effects are neglected. A constant electric field $\mathbf{E}_z$ is applied along the z-axis. In this scheme, we consider the photorefractive recording mechanism of dynamic gratings, i.e., the creation of an internal electric field $\mathbf{E}_{sc}$ by an unbalanced charge photoinduced by the light [13, 14]. This field is spatially modulated in accordance with the light interference pattern and is directed along the x-axis: $\mathbf{E}_x = \mathbf{E}_{sc}$ in Fig. 1.

In the case of a 2D cell, the orientational electro-optical effect is invoked by the transverse bend deformation, which is described only by the elasticity constant K_1. This electro-optical effect is commonly referred to as the S-effect. LC molecules have a definite initial orientation determined by the conditions of molecular orientation at the surface. Let θ_0 denote the initial inclination angle of the LC director with respect to the z-axis in the cell bulk. In particular, $\theta_0 = 0$ for the initial homeotropic orientation of molecules in the cell, and $\theta_0 = \frac{\pi}{2}$ for the planar orientation.

Consider the effects connected with the presence of a tangential electric field $\mathbf{E}_x = \mathbf{E}_{sc}$ that arises as a result of photo-induced charges under the action of a spatially inhomogeneous light beam. In this case, the LC molecules become reoriented under the action of the total field $\mathbf{E}$, which is defined as the sum of two vectors, $\mathbf{E} = \mathbf{E}_z + \mathbf{E}_x$. Consider the effects in the stationary state. This approach makes it possible to estimate the magnitude of the internal field $\mathbf{E}_x$ that has to be formed in the NLC by means of photo-induced mechanisms.

Anisotropy in NLCs is characterized in accordance with optically positive uniaxial crystals. The birefringence value is described with the help of the optical indicatrix ellipsoid, which determines the values of the refractive indices for the ordinary and extraordinary wave polarizations. Light beams with the ordinary and extraordinary polarizations pass through the nematic layer together, but acquire different phase incursions, $2\pi n_o L/\lambda$ and $2\pi n_e(\theta)L/\lambda$, with some phase delay between them. In the case of S-effects, only the rotation of the LC director in the (x, z)-plane is taken into account, and the twist effect is neglected. Under such conditions, the value of the refractive index for the ordinary wave does not change and is equal to $n_0 = n_\perp$. At the same time, the value of the refractive index for an extraordinary wave depends on the angle θ: $n_e(\theta = 0) = n_\perp$ for the homeotropic orientation, and $n_e(\theta = \frac{\pi}{2}) = n_\parallel$ for the planar one, where $n_\perp$ and $n_\parallel$ are the principal values of the refractive index. The optical anisotropy of nematic NLCs is evaluated by the difference $\Delta n = n_e(\theta) - n_o$ [3].

If an electric field $\mathbf{E}$ acts in the cell at an angle θ with respect to the z-axis, the LC molecules reorient so that the director vector becomes directed along the electric field vector, $\mathbf{d} \parallel \mathbf{E}$. A specific feature of the orientational electro-optical effect in NLCs is that the orientation of the crystal optical axis changes under the action of the net electric field. Thus, if the director reorients, the optical indicatrix ellipsoid rotates.

At the cell output, the difference δ between the phase incursions for the ordinary and extraordinary laser beams is equal to [2, 3, 23, 24]

$$\delta = \frac{2\pi L}{\lambda}\,[n_e(\theta) - n_0], \tag{1}$$

where λ is the light wavelength. The extraordinary light refractive index $n_e(\theta)$ depends on the angle of director reorientation θ with respect to the z-axis, which is described by the following formula (see [3]):

$$n_e(\theta) = \frac{n_\parallel n_\perp}{\sqrt{n_\parallel^2 \cos^2\theta + n_\perp^2 \sin^2\theta}}. \tag{2}$$

2.2. Intensity variations in the first diffraction orders due to the orientational S-effect at the two-wave mixing in NLCs

An optical scheme of the two-wave mixing in an LC material is shown in Fig. 2. A beam from laser *1* falls on splitting plate *3* and forms two beams of equal intensity. Those beams are reflected from mirrors *4* and *5*, and combined at NLC cell *6*. The dynamic grating is recorded under the action of the interference field created by those two beams. When the voltage U (*7*) is applied across the cell; the voltage is measured using a voltmeter. As a result of the self-diffraction of the recording beams at the phase grating created by themselves and the diffraction of a weak test beam that is emitted by laser *2* and does not destroy the grating, besides principal beams *8*, *9*, and *10*, high-order beams are generated: of the first-order self-diffraction ($\{-1\}$ – *11*, $\{+1\}$ – *12*) and the first-order diffraction ($\{1\}$ – *13*). The first-order intensities are measured using photodiodes *14* (for self-diffraction) and *15* (for diffraction) connected to a digital oscilloscope and a computer.

Consider characteristic changes in the intensity of the laser beam in the first diffraction orders for the self-diffraction of the laser beams and the diffraction of the test beam on the dynamic grating created as a result of the NLC director reorientation in the cell bulk. The change of the intensities in the first diffraction orders depends on the director rotation angle θ. Note that, according to our model, this reorientation occurs under the action of the superposition of the external, $\mathbf{E}_z$, and internal, $\mathbf{E}_x$, electric fields.

For the output intensity to the first self-diffraction order, the following formula was obtained [18]:

$$I_{\{-1\}} = I_{\{+1\}} = TI_0\,[J_1^2(\delta) + J_2^2(\delta)]. \tag{3}$$

The formula for the intensity in the first diffraction order for the diffraction of a test beam at a given phase grating is known from the theory of laser beam diffraction at acoustic waves:

$$I_{\{1\}} = TI_0\,J_1^2(\delta), \tag{4}$$

where the argument δ is described by formula (1) for the phase incursion $\delta(\theta, L)$ in the cell.

The above formulas were obtained in the Raman-Nath approximation for a purely local grating and provided equal input intensities of two pump laser beams, $I_{10} = I_{20} = I_0$. The quantities in formulas (3) and (4) are as follows: $I_{\{-1\}}$ and $I_{\{+1\}}$ are the output intensities of the laser beam in the orders $\{-1\}$ and $\{+1\}$, respectively, for the self-diffraction; $I_{\{1\}}$ is the output intensity of the test beam in the first diffraction order; T is the optical transmittance of the NLC cell; and J_1 and J_2 are the Bessel functions of the first kind and the first and second orders, respectively.

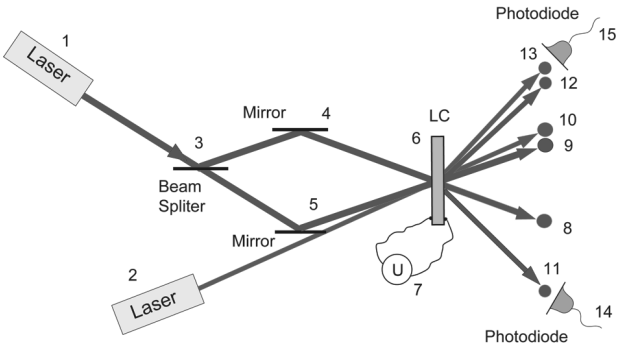

Fig. 2. Optical scheme of two-wave mixing in an LC cell: continuous frequency-doubled Nd:YAG laser *1* (green laser beam) is used for recording the dynamic grating and the self-diffraction of laser beams. Continuous He-Ne laser *2* (red laser beam) is used for diffraction testing at the given grating

2.3. Recording of dynamic gratings in NLCs via the photorefractive mechanism

A specific feature of the photorefractive mechanism at the creation of dynamic gratings in NLCs is the formation of an unbalanced charge under the action of a periodic interference field formed by two recording beams in the NLC cell [13, 14, 18]. It can be realized in nominally pure NLCs without impurities. In Fig. 1, the field created by the space charge is denoted as $\mathbf{E}_x$. As a result, there are two electric fields in the cell: the "external" electric field $\mathbf{E}_z$, which is created by applying the external voltage across the cell, and the "internal" tangential electric field $\mathbf{E}_x$. The total strength of those fields equals $\mathbf{E} = \mathbf{E}_z + \mathbf{E}_x$. If the electric field direction changes, the LC molecules reorient, and their long axes become aligned along the field direction. The dynamic grating is recorded owing to the spatial modulation of the director inclination angle θ. The modulation of the angle θ leads to the spatial modulation of the refractive index in the LC cell.

Figure 3 illustrates some examples of the refractive index modulation patterns calculated in the frame-

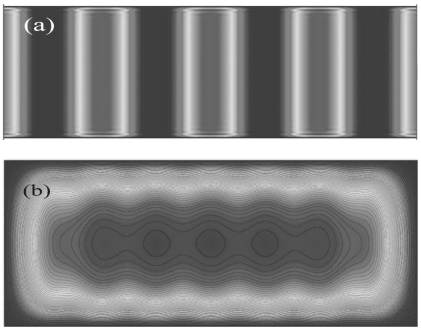

Fig. 3. Spatial modulation patterns of the refractive index (dynamic grating) in the NLC 5CB cell: interference field period $\Lambda = 50$ μm, cell thickness $L = 30$ μm, applied voltage $U = 5$ V, grating recording time $t = 0.15$ s (a); $\Lambda = 30$ μm, $L = 30$ μm, $U = 5$ V, $t = 10.1$ s (b)

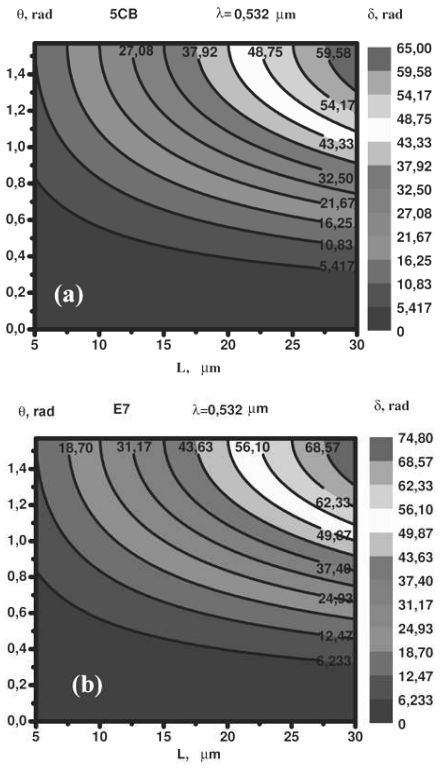

Fig. 4. Dependences of the maximum phase incursion δ (in radians) on the director orientation angle θ and the thickness L of the NLC cell with homeotropic orientation: 5CB (a), E7 (b). The director orientation angle θ is within an interval from 0 to $\frac{\pi}{2}$ with respect to the z-axis. The LC cell thickness L varies from 5 to 30 μm

work of the model of director reorientation under the action of an external electric field [25]. In Fig. 3, a, the grating has an optimal modulation depth, i.e., the difference between the maximum and minimum values of the refractive index. Figure 3, b demonstrates an almost "erased" grating with a small modulation depth. Such a grating is formed, if the spatial period of the interference pattern is small (as compared to the cell thickness), the applied voltage is high, or the duration of the light action is rather long.

We distinguish two types of dynamic grating recording:

- in a homeotropically oriented LC cell;
- in a planarly oriented LC cell.

3. Variation of the laser beam intensities at self-diffraction and diffraction at dynamic gratings in NLCs

3.1. NLC cells with initial homeotropic orientation

For a homeotropically oriented cell, the angle θ of director orientation rotation under the action of an electric field can vary from 0 to $\frac{\pi}{2}$ ($0 < \theta < \frac{\pi}{2}$). The value of the phase incursion difference δ from formula (1) determines the modulation depth of the dynamic grating. Figure 4 demonstrates the maps $\delta(L, \theta)$ describing the modulation depth variation at the maxima of the dynamic phase grating for an NLC with homeotropic orientation. The calculations were carried out for the NLCs 5CB ($n_{\parallel} = 1.7103$ and $n_{\perp} = 1.5271$ at the temperature $T = 24$ °C) and E7 ($n_{\parallel} = 1.7366$ and $n_{\perp} = 1.5258$ at $T = 25$ °C).

When calculating the output intensity in the first self-diffraction order, the numerical values of the phase incursion $\delta(L, \theta)$ from Eq. (1) were substituted into Eq. (3), and Eq. (2) was taken into account. The resulting plots are shown in Fig. 5. From this figure, one can see that the normalized values of the intensity (the diffraction efficiency) depend on the director rotation angle θ (the director is oriented along the direction of the net electric field **E**). Note that the diffraction efficiency has a pronounced maximum at $\theta \approx 0.5$ rad (≈28°) for a thin cell ($L = 5$ μm), and at $\theta \approx 0.2$ rad (≈11.5°) for a thick cell ($L = 30$ μm). Hence, the optimum depth of grating modulation depends on the director direction. Furthermore, the director rotation angle is small with respect to the initial orientation $\theta = 0$. At the same time, if the modulation depth δ is very large, periodic, but damped oscillations of the intensity take

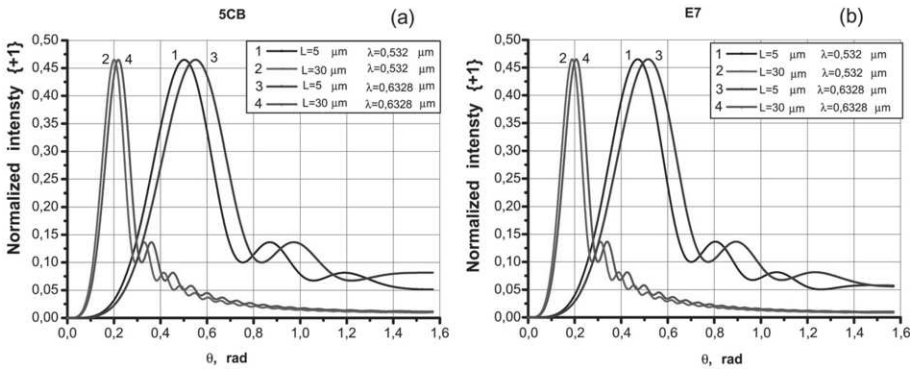

Fig. 5. Dependences of the normalized intensity (diffraction efficiency) of self-diffraction in the first diffraction order on the director rotation angle θ in the NLC cell with homeotropic orientation: 5CB (a), E7. (b) The calculations were carried out for the light wavelengths $\lambda = 0.532$ and 0.6328 μm, and NLC cell thicknesses of 5 and 30 μm

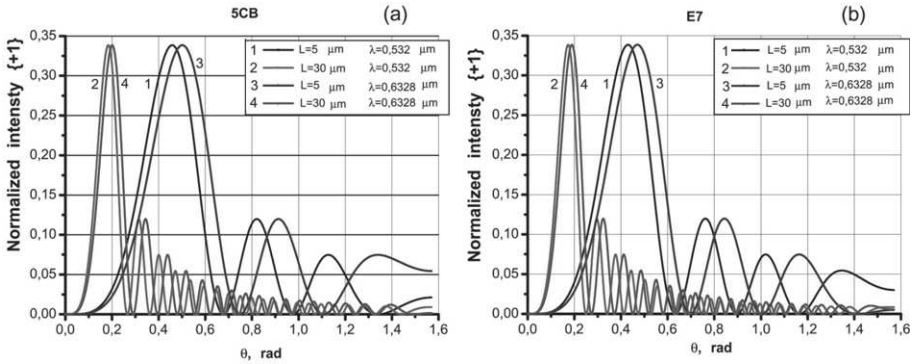

Fig. 6. Dependences of the normalized intensity (diffraction efficiency) in the first diffraction order on the director rotation angle θ for the test beam in the NLC with homeotropic orientation: 5CB (a), E7 (b). The light wavelengths and the cell thicknesses are the same as in Fig. 5

place. The maximum diffraction efficiency reaches a value of 46%.

Substituting the phase incursion values $\delta(L,\theta)$ from Eqs. (1) and (2) into Eq. (4), we obtain the value for the output intensity in the first diffraction order of the test laser beam. The corresponding characteristics for a homeotropic cell are shown in Fig. 6. By comparing it with Fig. 5, one can see that the behavior of the beam intensity in the first diffraction order is preserved: a well-pronounced maximum is observed at the same θ-values as in the self-diffraction case. The diffraction efficiency is reduced for the maximum magnitudes of the modulation depth of the grating, it drops and reaches zero in the minima. Thus, we obtained an interesting result: depending on the director rotation angle, the beam intensity in the first diffraction order acquires zero values, and the thicker the cell, the more the number of those "zeros".

3.2. NLC cells with initial planar orientation

Consider the variation of the dynamic grating modulation depth in an NLC cell with the initial planar orientation of molecules. In this case, the initial director angle $\theta = \frac{\pi}{2}$, and the angle θ changes in the opposite direction, i.e., from $\frac{\pi}{2}$ to 0 ($\theta = \frac{\pi}{2} \to 0$). Thus, the "background" has the maximum value

$$\delta_{\max}\left(L, \theta = \frac{\pi}{2}\right) = \frac{2\pi L}{\lambda}(n_e - n_o), \tag{5}$$

where $n_e = n_{\|}$ and $n_o = n_{\perp}$, and the grating amplitude decreases. Then it is the difference between the

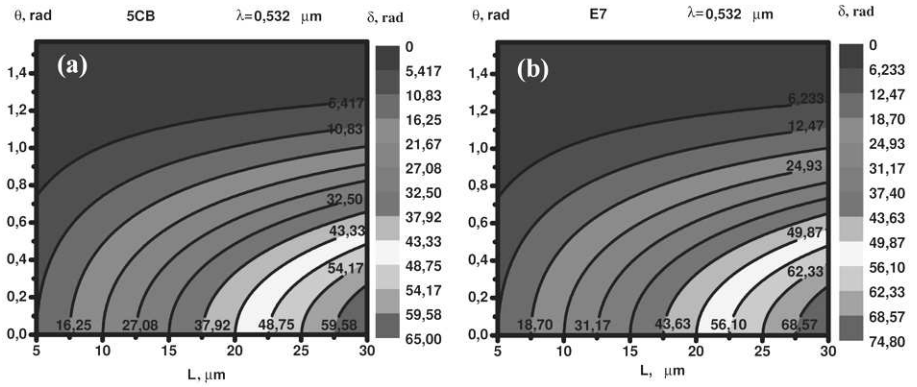

Fig. 7. Dependences of the maximum phase incursion δ_{pl} (in radians) on the director orientation angle θ and the thickness L of the NLC cell with planar orientation: 5CB (a), E7 (b). The director orientation angle θ is within an interval from 0 to $\frac{\pi}{2}$ with respect to the z-axis. The LC cell thickness L varies from 5 to 30 μm

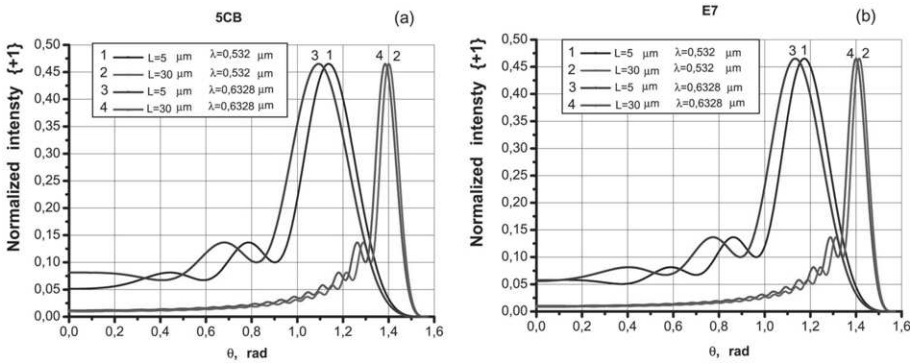

Fig. 8. Dependences of the normalized intensity (diffraction efficiency) of self-diffraction in the first diffraction order on the director rotation angle θ in the NLC cell with planar orientation: 5CB (a), E7. (b) The calculations were carried out for the light wavelengths $\lambda = 0.532$ and 0.6328 μm, and NLC cell thicknesses of 5 and 30 μm

"background" and $\delta(\theta)$ that determines the modulation depth of the dynamic grating:

$$\delta_{pl} = \delta_{\max}\left(L, \theta = \frac{\pi}{2}\right) - \delta(L, \theta). \tag{6}$$

Figure 7 illustrates the maps calculated for the dynamic grating modulation depth in the case of a planarly oriented cell. The figure demonstrates the opposite dependence of the maximum phase incursion values on the director inclination angle θ in comparison with Fig. 4 for the homeotropically oriented cell.

To calculate the output intensity in the first self-diffraction and diffraction orders, we should substitute the quantity δ_{pl} into formulas (3) and (4). The corresponding plots are shown in Figs. 8 and 9.

In comparison with the plots for a homeotropically oriented cell (Figs. 5 and 6), the general behavior of the diffraction efficiency dependence on θ survives: a pronounced maximum is observed, which gets narrower and shifts toward larger θ-values, as the cell thickness increases, as well as oscillations in the high-δ_{pl} region, where the diffraction efficiency for the test beam acquires zero values. Note once again that the deviations of the director from its initial orientation are too small for the maximum diffraction efficiency to be achieved. They are approximately the same as for a homeotropically oriented cell: $\Delta\theta \approx 1.6 - 1.1 = 0.5$ rad for $L = 5$ μm, and $\Delta\theta \approx 1.6 - 1.4 = 0.2$ rad for $L = 30$ μm.

3.3. Diffraction efficiency in NLC cells with high absorption

The calculations of the diffraction efficiency carried out in Sections 3.1 and 3.2 were performed in the

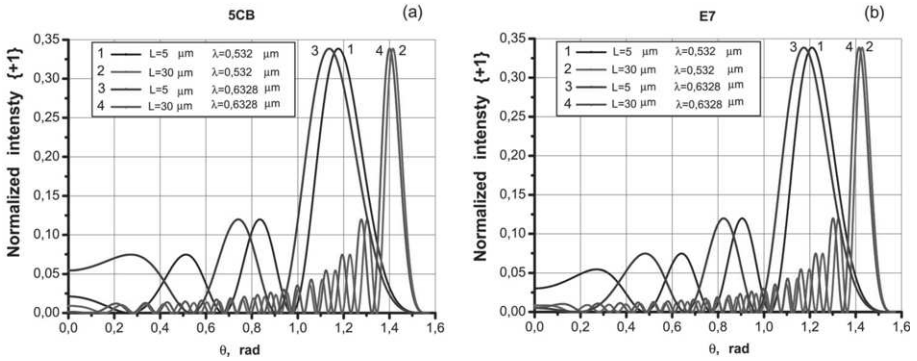

Fig. 9. Dependences of the normalized intensity (diffraction efficiency) in the first diffraction order on the director rotation angle θ for the test beam in the NLC with planar orientation: 5CB (a), E7 (b). The light wavelengths and the cell thicknesses are the same as in Fig. 8

approximation of low absorption in the NLC cells. This enabled us to reveal the main regularities in the variation of the beam intensities in the first orders, in particular, their dependence on the cell thickness L. But real NLC cells, as a rule, are characterized by a rather high absorption. As a result, the effective absorption thickness of the cell changes. It can be calculated using the formula (see, e.g., works [18–21])

$$L_{\text{eff}} = \frac{1-T}{\alpha}, \tag{7}$$

where α is the absorption coefficient of the cell. The parameter α is determined from experimental measurements of the cell optical density (or the optical transmittance T) at the examined wavelength. The transmittance T, the absorption coefficient α, and the optical density D are known to be related via the following relations:

$$T = 10^{-D}, \quad \alpha = \frac{D}{L}\ \ln\ 10. \tag{8}$$

To find the diffraction efficiency in the first self-diffraction and diffraction orders, the effective thickness L_{eff} is substituted for the thickness L in formula (1), and the quantity T is substituted into formulas (3) and (4).

Figures 10 and 11 demonstrate the calculated diffraction efficiencies for NLC cells with high absorption, $\alpha = 0.2\ \mu\text{m}^{-1}$; such α-values were obtained for NLC cells with nano-island films [21]. It can be seen that the effective thickness L_{eff} becomes very small in NLC cells with high absorption. Therefore, the plots even for thick cells are similar to the plots obtained for thin cells without absorption. There is another interesting feature: all plots of the diffraction efficiency obtained for various NLC thicknesses and various wavelengths almost coincide in the case of the cell with planar orientation (cf. Figs. 10, b and 10, d; and Figs. 11, b and 11, d). Therefore, thick cells with highly absorbing NLCs, despite their additional volume, have no gain in the diffraction efficiency. In this case, optimal and maximum η-values are observed even for thin cells.

4. Dependence of Diffraction Efficiency on Applied External Voltage

In the previous sections, we have obtained an important result: the output intensities calculated in the first diffraction orders for the NLC cells with the orientational birefringence S-effect reach their maximum values at certain director reorientation angles. As was pointed out above, in the case of the positive electro-optical effect in the NLC (for NLCs with $\Delta\varepsilon > 0$), the director becomes oriented along the acting electric field. In Fig. 1 with the schematic diagram of the 2D NLC cell, it is shown that, in the case of photorefractive mechanism, two electric fields act in the cell in perpendicular directions: the "external" electric field $\mathbf{E}_z$ created by applying a voltage to the cell substrates and the "internal" electric field $\mathbf{E}_x$ created due to the action of light with an inhomogeneous intensity distribution (the light interference field). The net electric field $\mathbf{E} = \mathbf{E}_z + \mathbf{E}_x$ is directed at an angle θ with respect to the z-axis (right panel in Fig. 1). The LC director is oriented exactly along the vector $\mathbf{E}$. By changing the rotation angle of the net field vector, it

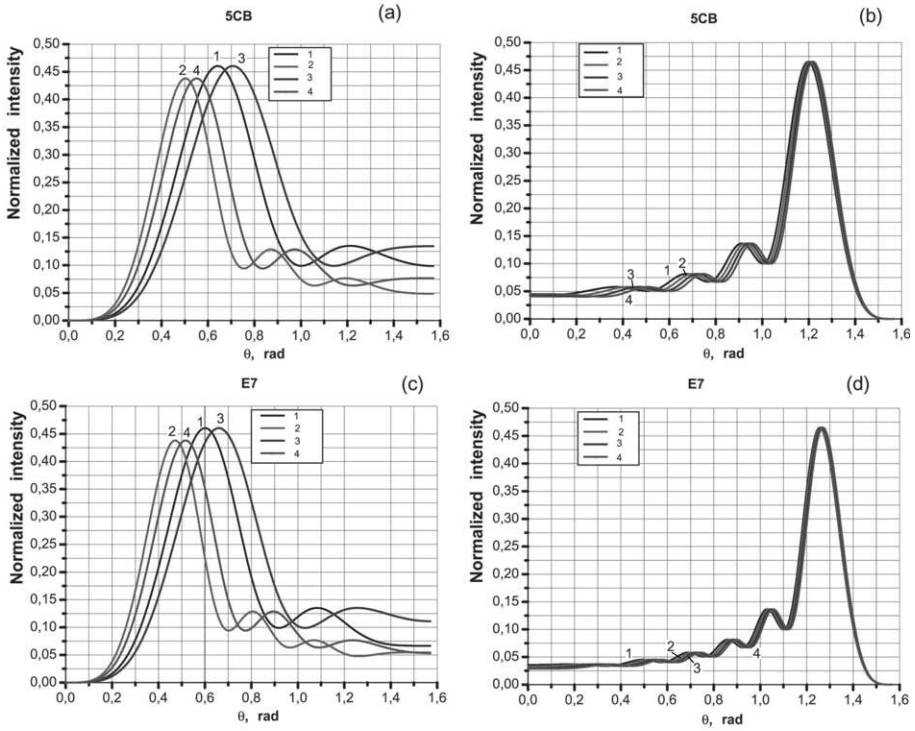

Fig. 10. Dependences of the diffraction efficiency in the first order of self-diffraction at a dynamic grating on the director rotation angle θ for NLC cells with the absorption coefficient $\alpha = 0.2\ \mu\text{m}^{-1}$: 5CB with homeotropic orientation (*a*), 5CB with planar orientation (*b*), E7 with homeotropic orientation (*c*), E7 with planar orientation (*d*). The curve calculation parameters are as follows: $L_{\text{eff}} = 3.16\ \mu$m, $L = 5\ \mu$m, $\lambda = 0.532\ \mu$m (*1*); $L_{\text{eff}} = 4.99\ \mu$m, $L = 30\ \mu$m, $\lambda = 0.532\ \mu$m (*2*); $L_{\text{eff}} = 3.16\ \mu$m, $L = 5\ \mu$m, $\lambda = 0.6328\ \mu$m (*3*); $L_{\text{eff}} = = 4.99\ \mu$m, $L = 30\ \mu$m, $\lambda = 0.6329\ \mu$m (*4*)

is possible to achieve the optimal (maximum) value for the efficiency of the diffraction of the output laser beams at the dynamic grating.

If we adopt that the internal field vector $\mathbf{E}_x$ is constant and determined by the processes of unbalanced charge formation (depending on the NLC type), then it is the variation of the applied voltage U that can change the angle θ for the net electric field. In experimental studies of the two-wave mixing, the dependence of the diffraction efficiency on U was observed. In particular, it has a pronounced maximum at a certain value U_0 [18–22].

Let us plot the dependence of the diffraction efficiency η on the applied voltage U, similarly to experimentally measured ones. The maximum diffraction efficiency is achieved at the fields E_x and E_z, when the director rotation angle is maximum, $\theta^{\max}$. According to Fig. 1, we obtain $\theta = \text{atan}(E_x/E_z)$, where E_x and E_z are the amplitudes of the internal (tangential) and external (normal), respectively, electric fields. We may assume that the applied voltage U affects only the magnitude of the external electric field E_z, whereas the magnitude of the internal field created by the space charge is determined only by the mechanisms of charge formation in a specific LC under the light action, i.e., we may put $E_x = \text{const}$. The corresponding system of equations looks like

$$\begin{aligned} E_z(U) &= \frac{U}{L} = E(U)\ \cos[\theta(U)], \\ E_x &= \text{const} = E_x^{\max} = E^{\max}\ \sin[\theta^{\max}], \end{aligned} \tag{9}$$

where $E_z(U)$ is the magnitude of the external electric field, which depends on the applied voltage U and leads to changes in the values of both the total field vector $E(U)$ and the corresponding director orientation angle $\theta(U)$. We can determine the magnitude of the constant field $E_x = E_x^{\max}$, if we know the angle $\theta^{\max}$ at which the diffraction efficiency is maximum.

Assume that the angle $\theta^{\max}$ is reached at the total field $\mathbf{E}^{\max}(U_0) = \mathbf{E}_z^{\max}(U_0) + \mathbf{E}_x^{\max}$ with a certain U_0-

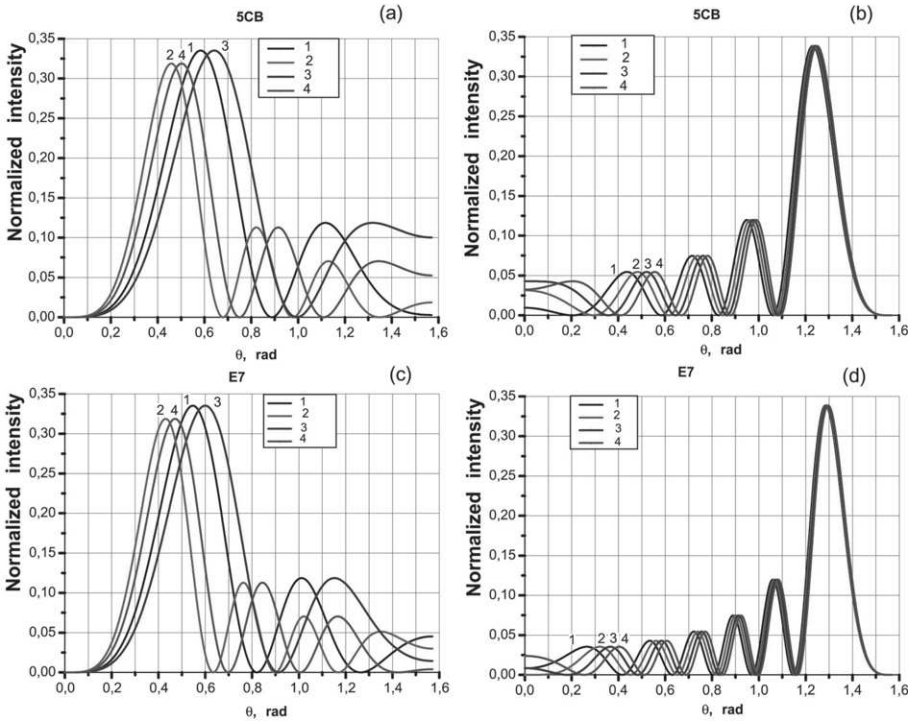

Fig. 11. Dependences of the diffraction efficiency in the first diffraction order of the test beam at a dynamic grating on the director rotation angle θ for NLC cells with the absorption coefficient $\alpha = 0.2\ \mu\text{m}^{-1}$: 5CB with homeotropic orientation (a), 5CB with planar orientation (b), E7 with homeotropic orientation (c), E7 with planar orientation (d). The curve calculation parameters are the same as in Fig. 10

value. One can see from system (9) that it is possible to exclude the field $E_z^{\max}(U_0)$ to get the formula for $E_x^{\max}$,

$$E_x^{\max} = \frac{U_0}{L} \tan\theta^{\max}. \tag{10}$$

Next, as in the previous calculations, the quantity $\theta(U)$ has to be substituted into formulas (1) and (2) for δ. Then, from system (9) and taking Eq. (10) into account, we obtain

$$\theta(U) = \tan\left(\frac{U_0}{U} \tan\theta^{\max}\right). \tag{11}$$

In this formula, the value for U_0 can be taken from experimental data, and the value for $\theta^{\max}$ from calculated data, e.g., from Figs. 5–6 and 8–11.

Here is an example of such a calculation for 5CB cells with homeotropic and planar orientations. From the calculated plots for the diffraction efficiency, we determine $\theta^{\max}$ and, in accordance with our model, assume $\theta^{\max} = \text{atan}\left(\frac{1}{E_z/E_x}\right)$, at which the maximum diffraction efficiency is observed. For many experimental data (see, for example, works [18–22]), the value of U did not exceed 15 V for cells of various thicknesses. But the U_0-value at the maximum diffraction efficiency in the first order was observed in most cases at about 3 V. Let us take $U_0 = 3$ V in our further calculations. The results are shown in Fig. 12.

Note that, in real cells with absorption, the effective cell thickness for a light beam is $L_{\text{eff}} < 5\ \mu$m, as a rule. Therefore, the curves for $L = 30\ \mu$m are presented only for comparison. But one can see that, for both initial orientations of LC molecules, a clear maximum is observed at $U = 3$ V. This is exactly the value that we chose for U_0.

Note also the difference between the plots for cells with homeotropic and planar orientations. For the homeotropic orientation (Figs. 12, a and b), several maxima of the diffraction efficiency are observed at voltages lower than U_0 ($U < U_0$). Such maxima were really observed in experiments with homeotropically

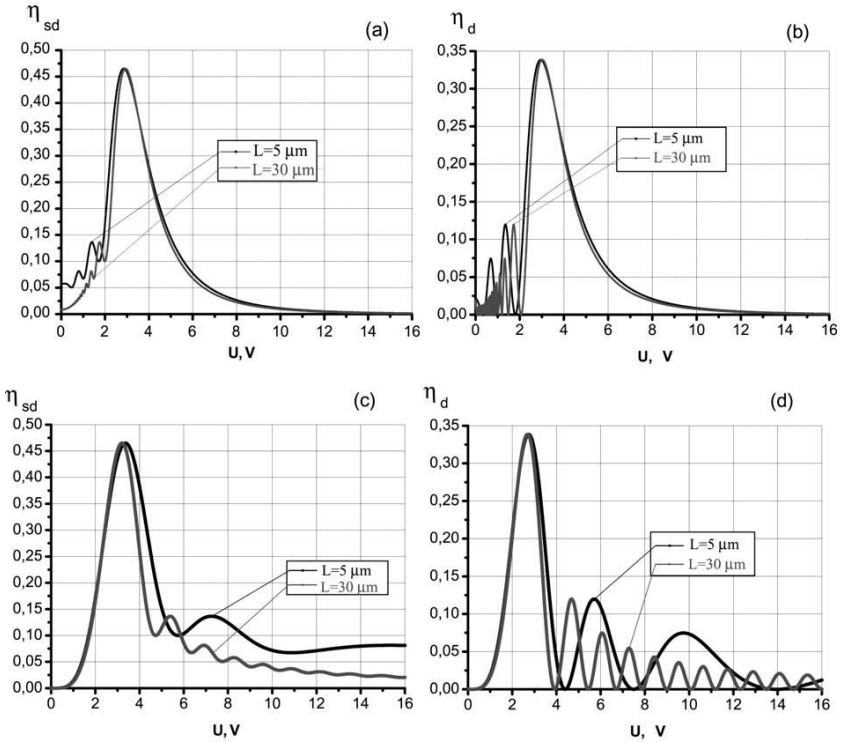

Fig. 12. Dependences of the diffraction efficiency on the magnitude of the applied voltage U in the first self-diffraction order (η_{sd}, panels a and c) and the first diffraction order for the test beam (η_d, panels b and d), for the homeotropic (panels a and b) and planar (panels c and d) orientations of LC 5CB. $L = 5$ (black curves) and 30 μm (red curves). Cells "with no absorption": $T = 1$, $L_{\text{eff}} = L$

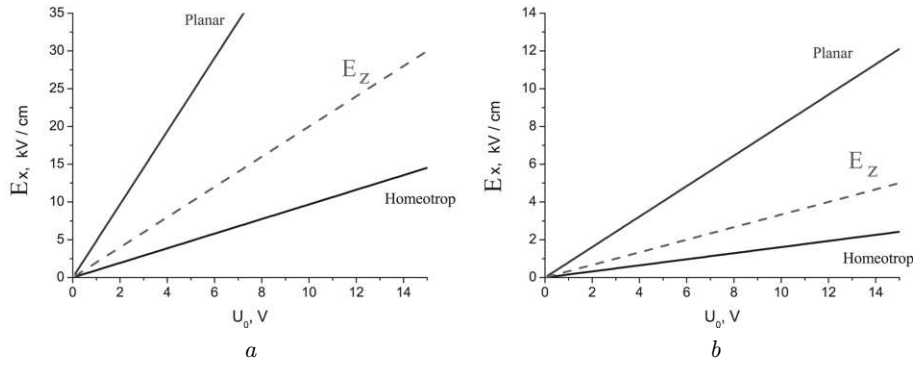

Fig. 13. The dependence of the strength E_x of the internal field generated by the space charge in LC 5CB cells on the voltage U_0 at which the maximum diffraction efficiency is observed. For comparison, the corresponding dependence for the external field E_z is plotted (the red dashed line). The cell thickness $L = 5$ (a) and 30 μm (b)

oriented cells. In addition, the value of η gradually decreases, as U increases, and, at $U > 6$ V, η becomes negligibly small. At the same time, for the planarly oriented cell (Figs. 12, c and d), the diffraction efficiency remains substantial in a wide range of voltages: many maxima of η are observed at $U > U_0$. This difference in the behavior of η can be used to identify the prevailing initial orientation of LC molecules in the cell.

Hence, the results of our calculations of the diffraction efficiency dependence on the magnitude of the external voltage applied across the cell are in the to-

tal agreement with the experimental data. Since our model was developed making allowance for the induction of an internal tangential electric field E_x in the cell at its illumination with an interference pattern with a non-uniform intensity distribution, the main conclusion can be drawn that such a space charge field is really formed inside the cell.

With the help of formula (10), let us evaluate the maximum strength E_x of the internal field generated by the space charge (see Fig. 13). In Fig. 13, *a*, the results of calculations for a cell with the thickness $L = 5$ μm are shown. For comparison, the magnitude of the external electric field $E_z = U_0/L$ in a cell with the same thickness is also plotted. One can see that the internal electric field in the homeotropically oriented cell is at least two times lower in comparison with E_z. At the same time, much higher values of E_x in comparison with E_z are required to obtain the maximum diffraction efficiency in the planar oriented cell.

Figure 13, *b* demonstrates the results obtained for the experimental NLC cell with absorption: the cell had the thickness $L = 30$ μm, and the absorption coefficient $\alpha = 0.2$ μm^{-1}. For such cells, the optical characteristics are calculated with regard for L_{eff} in the formulas for the diffraction efficiency, and the real call thickness value should be used when calculating the electric field. According to formula (7), $L_{\text{eff}} = 4.9875$ μm ≈ 5 μm for the experimental cell, so we can accept the already calculated value $\theta^{\max}$ for $L = 5$ μm. One can see from the plot that the electric fields in such a real cell are six times lower. Hence, to obtain the maximum diffraction efficiency, much lower internal electric fields are required.

We emphasize once again that, in accordance with our model, the field created by the internal space charge acquires a single value and does not depend on U. The magnitude of $E_x^{\max}$ can be determined from the experiment by measuring the dependence $\eta(U)$, as we did in this subsection when determining the U_0-value, which is the maximum value in this dependence.

5. Conclusions

In this paper, a model for calculating the intensities of laser beams in the first diffraction orders at the two-wave mixing of laser waves in the nematic liquid crystal cells has been developed. Both the intensities in the self-diffraction mode for the recording laser beams and for the test laser beam at its diffraction at the dynamic grating are calculated. The modulation depth of the dynamic phase grating is calculated under the assumption that the NLC director changes its orientation under the action of the electric field, which leads to a variation of the optical birefringence in the NLC cell.

The calculated parameters of the diffraction efficiency agree with the experimental data obtained while studying the two-wave mixing in the NLC. In particular, the following experimental results are obtained:

(i) dynamic gratings are recorded in nominally pure NLCs, if an external electric voltage is applied;

(ii) self-diffraction and diffraction of laser beams are observed for cells with both homeotropic and planar orientations of LC molecules;

(iii) a pronounced maximum is observed in the dependence of the diffraction efficiency on the applied voltage; i.e., there is an optimal value of U_0 at which the diffraction efficiency is maximum.

In the framework of the developed model, the obtained experimental results can be explained by engaging the photorefractive mechanism of dynamic grating recording. Its specific feature consists in the generation of an unbalanced charge and the formation of the corresponding internal electric field under the action of a light interference pattern. As a result, the net electric field giving rise to the director reorientation consists of the external electric field created by applying a voltage across the cell and the internal electric field created by the space charge arising under the light action. If the internal field is assumed to be independent of the applied voltage U, then the change of U changes the magnitude of the external field vector and induces the rotation of the net electric field vector. As a result, the NLC director becomes reoriented along the vector of the total electric field acting in the cell.

In accordance with our model, it is found that the diffraction efficiency reaches a maximum at a certain value of the director rotation angle. This rotation angle is small with respect to the initial orientation of the molecules. The obtained dependencies also made it possible to explain the existence of the optimal voltage value U_0 at which the diffraction efficiency achieves its maximum value.

Interesting dependences are obtained for the first time for the diffraction efficiency in NLC cells with

high optical absorption. In this case, the effective cell thickness acquires small values even for thick cells. Therefore, the output intensities calculated in the first diffraction orders are only slightly different for thin (∼5 μm) and thick (∼30 μm) cells. For planar oriented cells, all calculated dependences – for thin and thick cells, and for various wavelengths of recording laser beams – coincide.

The obtained results are fundamental for the design and development of practical NLC-based elements, such as light modulators and sensors.

The authors are grateful for sponsoring this work by the National Academy of Sciences of Ukraine (grants 1.4.B/219 and 1.4B/210). S. Bugaychuk also thanks the University of Lille, the Laboratory of Physics of Lasers, Atoms and Molecules (PhLAM), and the French programme PAUSE for financial support.

1. J.C. Jones. *Liquid Crystal Displays* (Taylor and Francis Group, 2018).
2. Iam-Choon Khoo, *Liquid Crystals* (John Wiley and Sons, 2022).
3. L.M. Blinov. *Structure and Properties of Liquid Crystals* (Springer, 2011).
4. A. Lininger, A.Y. Zhu, J.-S. Park, G. Palermo, S. Chatterjee, J. Boyd, F. Capasso, G. Strangi. Optical properties of metasurfaces infiltrated with liquid crystals. *Proc. Natl. Acad. Sci. USA* **25**, 20390 (2020).
5. G. Klimusheva, S. Bugaychuk, Yu. Garbovskiy, O. Kolesnyk, T. Mirnaya, A. Ishchenko. Fast dynamic holographic recording based on conductive ionic metal-alkanoate liquid crystals and smectic glasses. *Opt. Lett.* **31**, 235 (2006).
6. Fengfeng Yao, Rongqu Hong, Yunpen Gao, Zhaoheng Wang, Yanbo Pei, Chunfeng Hou *et al.* Dynamic holographic liquid crystal device containing nanoscale CuPc film. *Liq. Cryst.* **46**, 1108, (2019).
7. S. Residori, U. Bortolozzo, J.P. Huignard. Liquid crystal light valves as optically addressed liquid crystal spatial light modulators: optical wave mixing and sensing applications. *Liq. Cryst. Rev.* **6**, 1 (2018).
8. J. Parka, T. Grudniewski, Yu. Kurioz, R. Dabrowski. Optically addressed holographic gratings in LC cells with different layers and high optical anisotropy liquid crystals. *Opto-Electron. Rev.* **12**, 317 (2004).
9. S.B. Abbott, K.R. Daly, G. D'Alessandro, M. Kaczmarek, D.C. Smith. Hybrid liquid crystal protorefractive system for the photorefractive coupling of surface plasmon polaritons. *J. Opt. Soc. Am. B* **29**, 1947 (2012).
10. U. Bortolozzo, S. Residori, J.P. Huignard. Beam coupling in photorefractive liquid crystal light valves. *J. Phys. D* **41**, 224007 (2008).
11. D. Psaltis, D. Brady, XG. Gu, S. Lin. Holographpy in artificial neural networks. *Nature* **343**, 325 (1990).
12. F. Laporte, J. Dambre, P. Bienstman. Simulating self-learning in photorefractive optical reservoir computers. *Sci. Rep.* **11**, 2701 (2021).
13. J. Frejlich. *Photorefractive Materials: Fundamental Concepts, Holographic Recording and Materials Characterization* (Wiley-Interscience Publication, 2007).
14. F. Simoni, L. Lucchetti. Photorefractive Effects in Liquid Crystals. in *Photorefractive Materials and Their Applications 2. Edited by P. Günter, J.-P. Huignard* (Springer, 2007), p. 571.
15. P. Korneychuk, O. Tereshchenko, Yu. Reznikov, V. Reshetnyak, K. Singer. Hidden surface photorefractive gratings in a nematic liquid crystal cell in the absence of a deposited alignment layer. *J. Opt. Soc. Am. B* **23**, 1007 (2006).
16. Y.J. Liu, X.W. Sun. Holographic polymer-dispersed liquid crystals: materials, formation, and applications. *Adv. Optoelectron.* **2008**, 684349 (2008).
17. R.L. Sutherland, B. Hagan, W.J. Kelly, B. Epling. Switchable polymer-dispersed liquid crystal optical elements. *US Patent* No. US007265903B2, Sep. 4, 2007.
18. S. Bugaychuk, A. Iljin, O. Lytvynenko, L. Tarakhan, L. Karachevtseva. Enhanced nonlinear optical effect in hybrid liquid crystal cells based on photonic crystal. *Nanosc. Res. Lett.* **12**, 1 (2017).
19. S. Bugaychuk, L. Viduta, A. Gridyakina, H. Bordyuh, V. Styopkin, L. Tarakhan, V. Nechytaylo. Faster nonlinear optical response in liquid crystal cells containing gold nano-island films. *Appl. Nanosci.* **10**, 4965 (2020).
20. S. Bugaychuk, L. Viduta, L. Tarakhan, V. Cherepanov, A. Gridyakina, H. Bordyuh, A. Iljin, V. Nechytaylo. Optical linear and nonlinear properties of hybrid liquid crystal cells containing gold island films. *Mol. Cryst. Liq. Cryst.* **696**, 93 (2020).
21. S. Bugaychuk, S. Kredentser, Y. Kurioz, A. Gridyakina, H. Bordyuh, L. Viduta, V. Styopkin, D. Zhulai. Recording of dynamic and permanent gratings in composite LC cells containing gold nano-island films. *Mol. Cryst. Liq. Cryst.* **750**, 23 (2023).
22. Yu. Kurioz, S. Bugaychuk, S. Kredentser, H. Bordyuh, A. Gridyakina, V. Styopkin, L. Viduta. Effect asymmetry of diffraction efficiency in LC cells with different command surfaces. *Mol. Cryst. Liq. Cryst.* **748**, 29 (2022).
23. A.S. Sonin. *Introduction to the Liquid Crystal Physics* (Nauka, 1983) (in Russian).
24. P.G. De Gennes, J. Prost *The Physics of Liquid Crystals* (Oxford University Press, 1993).
25. S. Bugaychuk, V. Mystetskyi. Kinetics of dynamic refractive index gratings in nematic liquid crystals in spatially inhomogeneous electric fields. *Mol. Cryst. Liq. Cryst.* **747**, 64 (2022).

Received 30.06.23.
Translated from Ukrainian by O.I. Voitenko

В.А. Мистецький, С.А. Бугайчук

КЕРУВАННЯ ІНТЕНСИВНІСТЮ ЛАЗЕРНОГО ВИПРОМІНЮВАННЯ У РІДКОКРИСТАЛІЧНИХ ВЕНТИЛЯХ ПРИ ЗАПИСІ ОБ'ЄМНОЇ ДИНАМІЧНОЇ ҐРАТКИ

Експериментальні дослідження номінально чистих нематичних рідких кристалів (НРК) підтверджують запис динамічних голографічних ґраток у комірках як з гомеотропною орієнтацією, так і з планарною. Пояснення можна знайти, виходячи із фоторефрактивного механізму запису ґратки, особливістю якого являється формування нерівноважного заряду на поверхні підкладинки комірки під дією просторово неоднорідного світлового поля. Поява внутрішнього тангенціального електричного поля (вздовж підкладинок комірки), разом із зовнішнім електричним полем, що прикладається нормально до підкладинок комірки, відкриває додаткові можливості у керуванні напрямку вектора результуючого електричного поля. В даній роботі розроблена і аналізується модель зміни інтенсивностей лазерних променів при їх самодифракції і дифракції на динамічній ґратці, створеній в НРК. Динамічна фазова ґратка формується завдяки орієнтаційному механізму двозаломлення в НРК при двопучковій взаємодії лазерних променів, що утворюють просторово періодичну інтерференційну картину діючого світлового поля. Результати проведених розрахунків вихідних інтенсивностей лазерних променів в перших порядках самодифракції і дифракції добре узгоджуються з експериментальними вимірюваннями. Зокрема, вони пояснюють залежність дифракційної ефективності від величини зовнішньої прикладеної напруги, що має добре виражений максимум.

Ключові слова: нематичні рідкі кристали, двопучкова взаємодія, динамічні ґратки, дифракційна ефективність.